

Globular Clusters of the Galaxy: Chemical Composition vs Kinematics

V. A. Marsakov, V. V. Koval', M. L. Gozha
 Southern Federal University, Rostov-on-Don, Russia
 e-mail: marsakov@sfnedu.ru, litlevera@rambler.ru, gozha_marina@mail.ru

accepted 2019, Astrophysical Bulletin, Vol. 74, No. 4, pp. 403–423

Abstract

A comprehensive statistical analysis of the relationship between the chemical and spatially kinematic parameters of the globular clusters of the Galaxy has been performed. The data of the authors compilation catalog contain astrophysical parameters for 157 clusters and the relative abundances of α -elements for 69 clusters. For 121 clusters, the data are supplemented by spatially kinematic parameters taken from the literature. The phenomenon of reddening of horizontal branches of low-metal accreted globular clusters is discussed. We consider the contradiction between the criteria for clusters to belong to the subsystems of the thick disk and the halo in terms of chemical and kinematic properties. It consists in the fact that, regardless of belonging to the galactic subsystems by kinematics, almost all metallic ($[\text{Fe}/\text{H}] > -1.0$) clusters are located close to the center and plane of the Galaxy, while among the less metallic of both subsystems there are many distant ones. Differences in the abundances of α -elements in the stellar objects of the Galaxy and the surrounding low-mass dwarf satellite galaxies confirm the wellknown conclusion that all globular clusters and field stars of the accreted halo are remnants of galaxies of higher mass than the current environment of the Galaxy. A possible exception is a distant low-metal cluster with low relative abundance of α -elements Rup 106.

Key words: Galaxy: structure—globular clusters: general.

1 Introduction

Globular clusters are one of the oldest objects in the Galaxy, and therefore cause great interest in connection with the possibility to understand how the formation and early evolution of the Milky Way happened. Until recently, all globular clusters were considered to be typical representatives of their own galactic halo, that is, formed from a single protogalactic cloud at the initial stages of the formation of the Galaxy. However, it was subsequently shown that some of the clusters most likely landed on our Galaxy from decaying satellite galaxies. This discovery roughly coincided in time with the emergence of the theory that massive galaxies like ours are formed in the early stages of their evolution as a result of the continuous accretion of dwarf galaxies. In paper [1] (hereinafter MKG19) we provide a list containing 22 supposedly accreted clusters, and references to works in which this is stated. Among them are ten clusters lost by the dwarf galaxy Sagittarius (Sgr), seven clusters-by the Canis Major galaxy (CMa) and five clusters-by other satellite galaxies.

A characteristic feature of such clusters was the phenomenon of abnormally reddened horizontal branches, not corresponding to their low metallicity, and often large distances from the galactic center. The excess of stars on the red part of the horizontal branch at low metallicity appears in the case of a younger age of the cluster, so they were initially considered “young”. It is on these grounds that they were selected when researchers wanted to explore them in more detail. It is generally accepted that such clusters form a subsystem, which, according to the chosen dominant feature, is called the “young halo”, “external halo” or “accreted halo” (see, for example, paper [2] and references therein). But the

remaining genetically related clusters, which are believed to have formed from a single protogalactic cloud, are divided into two subsystems: the thick disk and the halo itself. The separation is due to the metallicity distribution of the clusters, which reveals a sharp dip in the vicinity of $[\text{Fe}/\text{H}] \approx -1.0$ (see, for example, the papers [2],[3]). At the same time, more metal-rich clusters are considered representatives of the thick disk subsystem of the Galaxy.

For a long time it was believed that the formation of all stars in each cluster occurred simultaneously, and therefore the abundances of all chemical elements in the stars must correspond to the abundances in the primary protoclouds of these clusters. But then found out, that in all clusters the self-enrichment was happening, which changed abundances of some chemical elements (see, for example, paper [4] and references therein). In general, the abundances of only those chemical elements that are involved in proton capture processes occurring during hydrostatic helium combustion in the center or in the layer sources of asymptotic giant branch (AGB) stars turned out to be distorted. Mainly, these processes in AGB stars decrease the relative abundances of primary α - elements (oxygen and to a lesser extent magnesium) and increased sodium and aluminum. When such a star loses its envelope at a later stage of evolution, these elements enter the interstellar medium of the cluster. As a result, new generations of stars in it are with a changed chemical composition. The average abundances of the remaining chemical elements in cluster stars remain almost primary (see, for example, paper [5] and references therein). This allows us to use these abundances to understand the evolution of the Galaxy in the early stages of its formation.

Since globular clusters belonging to different subsystems were formed from interstellar matter that has experienced different scenarios of chemical evolution, it can be expected that the relative abundances of chemical elements in clusters of different nature will differ. This work is devoted to a comparative statistical analysis of the relationship of the relative abundances of α -elements with the spatially kinematic characteristics of globular star clusters belonging to different subsystems of the Galaxy, in order to clarify their nature and verify the results of our previous work [1] (MKG19), where the same problem was investigated for almost half the number of clusters with known kinematic data, and of lower quality.

2 INITIAL DATA

Our catalog was created on the basis of the computer version of Harris [6] compilation catalog, which includes all measured values for 157 globular star clusters of the Galaxy. These data are supplemented by the relative abundances of 28 chemical elements in the stars of 69 globular clusters from 101 papers published from 1986 to 2018. References to these papers can be found in the on-line catalog, which is the Appendix in MKG19, which gives a detailed description of the procedure for averaging the relative abundances and their errors, and also shows that the external convergence of the definitions of the chemical composition of different authors lies in the range $\langle\sigma[\text{el}/\text{Fe}]\rangle = (0.06 - 0.16)$. Moreover, the values of the external convergence of the definitions of the relative abundances of chemical elements in clusters turned out to be only slightly more than the variances of the abundances in cluster stars declared by the authors of the primary papers. This indicates the absence of significant discrepancies between the definitions of the abundances by different authors and the possibility of using our compiled abundances of chemical elements for statistical analysis of the chemical composition of clusters belonging to different subsystems of the Galaxy. Here we consider the behavior of relative abundances in globular clusters of only four chemical elements: magnesium, silicon, calcium and titanium as the most informative in terms of describing the evolution of the early Galaxy. Most attention will be paid to the relative abundances of calcium and titanium. In the visible spectrum, these two chemical elements have many lines, and their abundances are quite reliably determined. The choice of these elements is due to the fact that the average relative abundances of both primary α -elements — oxygen and magnesium — in the course of cluster evolution decrease compared to their abundances in primary proto-clouds. And the abundances of another α -element — silicon — are determined for a smaller number of clusters and are not at all determined for field

stars and dwarf satellite galaxies, which we use for comparison.

For all 157 globular clusters, we calculated the rectangular coordinates from positions and distances from [7], and for 115 of them—from [8]. We supplemented the data for the last 115 clusters with cylindrical velocity components, taking them from the authors of [8], and for the clusters Ter 4, Pal 3, Pal 5, Pal 13, NGC6528 and NGC7006 calculated them from their proper motions, radial velocities and distances from [7]. As a result, the number of clusters with known velocities increased by more than two-thirds compared to our previous work MKG19 and totals 121 objects. Among them are 63 clusters (45 – in MKG 19) with the found abundances of chemical elements. The rectangular velocity components in a cylindrical coordinate system, the center of which is placed in the center of the Galaxy, were obtained on the basis of modern deep surveys (see studies [8], [9]). Previously, cross-identification was performed for objects of the catalogs USNO-B1, (U. S. Naval Observatory A1.0 catalogue), 2MASS (Two Micron All-Sky Survey), URAT1 (The First U. S. Naval Observatory (USNO) Astrometric Robotic Telescope Catalog), ALLWISE (The Wide-field Infrared Survey Explorer et IPAC), UCAC5 (New Proper Motions using GaiaDR1) and GaiaDR1 (based on the Tycho-Gaia Astrometric Solution) with subsequent reduction to the system Gaia DR1 TGAS (Tycho Gaia Astrometric Solution). In so doing, the difference of epochs was up to 65 years, the velocity of the Sun relative to the galactic center was taken equal to $(U, V, W)_{\odot} = (-10, 12 + 237, 7)$ km s⁻¹, and its galactic distance — $R_{GC} = 8.3$ kpc. The average internal error declared by the authors for determining the components of spatial velocities is approximately 17 km s⁻¹. Elements of galactic orbits calculated from these velocities are also taken from [8]. We used the latter here solely to distinguish clusters that have orbital points further than 15 kpc from the galactic center (see below for more details). The ages of clusters we took from papers [10] and [11].

To facilitate the understanding of the text and detail of the figures, we have compiled a Table in which we have included the parameters of globular clusters used in this work, as well as indicated the belonging of clusters to a particular subsystem or group. The columns of the Table contain the following information: (1) — cluster name, (2)–(4) — heliocentric coordinates (x, y, z) in the right-hand orthogonal system in kiloparsecs, (5) — metallicity $[\text{Fe}/\text{H}]_{\text{H}}$ according to the Harris catalogue. Columns (6)–(8) contain the iron abundances we found, as well as the relative abundances of two and four α -elements, further velocity components in the cylindrical coordinate system: V_R , V_{Θ} , V_Z , where the component V_R is directed to the anti-center of the Galaxy, V_{Θ} — in the direction of galactic rotation, V_Z — to the North pole of the Galaxy (see above for details on the sources of cluster positions and velocities). This is followed by Galactocentric distance (12), absolute magnitude (13), and color index HBR¹. The last two columns, (15) and (16), show the clusters belonging to the galactic subsystems: T, TD and H are thin disk, thick disk and halo, respectively, and the clusters belonging to the groups: i – internal: located at a distance (or apogalactic radii of their orbits) less than 8 kpc, o – distant: located at a distance or have radii of orbits more than 15 kpc, r – retrograde, with velocity of azimuthal components less than zero, a – accreted, for which the works of other authors prove their extragalactic origin, t – genetically related—clusters that did not fall into any of the last three groups. For comparison, we used the catalog [12], which gives metallicity, relative abundances of α -elements and components of spatial velocities for 785 stars of the galactic field in the entire range of metallicity of interest.

3 STRATIFICATION OF GLOBULAR CLUSTERS BY GALAXY SUBSYSTEMS

In [5] for the first time the stratification of globular clusters by subsystems of the Galaxy was carried out using not traditional criteria for metallicity and morphology of the horizontal branch, but by the components of their residual velocities, as has been done for field stars for a long time. In the

¹Morphological index, or horizontal branch color $\text{HBR} = (\text{B} - \text{R})/(\text{B} + \text{V} + \text{R})$, where B, V, R are respectively the number of stars at the blue end of the horizontal branch, in the instability band, and at the red end.

compilation catalog for 45 clusters cited in this work, the abundances of some chemical elements are found, and for 29 of them there is kinematic information. The authors found that most of the clusters by kinematics belong to the galactic halo, however, a significant number of clusters turned out to have disk kinematics, three of them—that of thin disk. More than a dozen clusters were included in the accreted halo, for which, according to the elements of their galactic orbits, different authors showed that they were most likely captured from several satellite galaxies, that is, of extragalactic origin.

It is clear that a single and sufficient criterion for stratification of globular clusters by subsystems of the Galaxy does not exist. To reliably classify a cluster as a particular subsystem, one should take into account many parameters characteristic of each subsystem, in particular, position, kinematics, metallicity, abundances of different chemical elements, age and morphology of the horizontal branch. Since we are going to study the differences in the chemical composition of clusters of different subsystems, here, as in the previous work, we used the kinematic criterion in which, according to the velocity components V_R , V_Θ , V_Z , the probabilities of clusters belonging to the subsystems of a thin disk, a thick disk, and a halo are calculated by the method described in [13]. This technique is similar to the technique used in the study [5], with only slightly different velocity dispersions in the subsystems. In both methods, it is assumed that the components of the spatial velocities of stars in each subsystem obey normal distributions. As the subsequent comparison showed, the belonging in the same clusters turned out to be different only in the case of differences in the input velocities—here they are more accurate. As shown by the subsequent comparison, the belonging of the clusters of the same name turned out to be different only in the case of differences in the input velocities—we have them more accurate. Since belonging to the subsystems are calculated from the residual velocities, we have reduced the azimuthal components of the cluster velocities to the rotation velocity of the centroid at the galactocentric distance at which the cluster is located. We took the rotation curve from the Galaxy model [8]. Taking into account the large distance of clusters, which leads to large errors in determining tangential velocities, and also taking into account that clusters do not concentrate to the galactic plane and do not participate in the general rotation of the galactic disk, as close stars of the field, for which the [13] method was developed, we performed a recurrent procedure when calculating the probabilities of falling clusters in a particular subsystem. In the second step, we assigned the velocity dispersions and the numbers of clusters in subsystems in the probability formulas such values as we obtained after the first step. This reduced the specified portion of objects in the subsystems of the thin and thick disks. Although the recalculation somewhat redistributed the belonging of a number of clusters that are kinematically in the transition zones between the thin and thick disks, as well as between the thick disk and the halo, but in general the composition of subsystems has changed insignificantly. To eliminate the ambiguity of individual stratification in paper [13] it is recommended to consider a star as belonging to a subsystem if the probability of its belonging to an alternative subsystem is at least two times less. As a result of this assumption, there is no stratification for a number of sample stars even with kinematic data. Such stars are usually referred to as intermediate. In view of the fact that we are interested in statistical regularities in subsystems, which can be identified only by a significant number of objects, we stratified all our globular clusters by subsystems, believing the sufficient criterion is simply a higher probability of belonging to any subsystem. The Table indicates the belonging to the galactic subsystems for those clusters, for which we have estimates of spatial velocities.

Fig. 1a presents the Tumre diagram “ $V_\Theta^2 - (U_R^2 + W_Z^2)^{0.5}$ ” for our globular clusters and field stars from the study [12]. The figure shows that objects demonstrating the kinematics of the subsystems of the same name occupy approximately the same areas on the diagram, although in [12] the technique slightly different from our one was used for field stars. The application of our technique showed that, from the kinematic parameters, for 84 clusters (40 in MKG 19) the probability of belonging to the halo is greater than to other subsystems. 34 clusters (28 in MKG 19) more likely belong to the thick disk, and three clusters (four in MKG19) turned out to be with the kinematics of the thin disk. We see that another model of the rotation curve of the Galaxy, more accurate estimates of the velocity, as well as a significantly increased number of velocity components, slightly reduced the number of clusters

in the thin disk, but the population of the thick disk increased by almost a quarter, and the number of halo clusters more than doubled. Note that a comparison of the velocity components showed a noticeable difference for the correlation coefficients of the same-named components $r = (0.6 - 0.7)$. And the differences in velocities, as shown by the test, are caused mainly by the refinement of their proper motions, and not the distances to the clusters. As a result, the subsystems did not have the same clusters in all cases. In particular, none of the three clusters with the thin disk kinematics (according to the results of this work) belonged to this subsystem in MKG19. In the thick disk, 17 clusters were common. Estimates of the velocities of about a dozen clusters have changed so that instead of a thick disk, as in the previous work, in the present work they fell into the halo. Significant differences in velocities should be noted. So, according to the data on velocities from paper [7] used in our previous work, the greatest velocity was for the cluster NGC 6553 $V_{\Theta} = 383 \text{ km s}^{-1}$ and now this value is 176 km s^{-1} . The azimuthal components of the velocities of two other clusters — Pal 6 and NGC 6284 — decreased as much, and for three clusters — NGC 4147, NGC 6144 and NGC 6723 — they increased. In Fig. 2a, it can be seen that among the clusters with the kinematics of the thick disk there was a significant number of such objects with rotational velocities around the galactic center even larger than those of the Sun. Two thick disk clusters (NGC 6496 and NGC 6528) have azimuthal velocities above 300 km s^{-1} at all. Four clusters with such large direct azimuthal velocities are also present in the halo. It is also seen that more than half of the halo clusters exhibit retrograde rotation around the galactic center. We believe that such clusters are highly likely to be of extragalactic origin. Indeed, according to the hypothesis of the monolithic collapse of the protogalaxy from the halo to the disk [14], the field stars and globular clusters genetically associated with the Galaxy cannot be in retrograde orbits.

Fig. 1b shows the distribution of clusters in the coordinates “the distance from the galactic plane (z) – the metallicity $[\text{Fe}/\text{H}]$ ”. In diagrams where spectroscopic determinations of other chemical elements are not used, the $[\text{Fe}/\text{H}]$ values were taken from the catalog [6], since it contains the metallicities for all clusters. Large circles in the figure indicate clusters belonging, according to kinematic characteristics, to a thin disk (empty), a thick disk (red) and a halo (dark gray), and asterisk are unstratified clusters, that is, clusters with unknown velocities. The most noticeable detail in the figure is the high concentration of metallic ($[\text{Fe}/\text{H}] > -1.0$) clusters near the galactic plane, regardless of whether it belongs to the subsystem of the Galaxy determined by kinematic criteria. As the test showed, the maximum distance of the orbit points of all² metal clusters were less 5 kpc, while for a significant part of small metal clusters $Z_{max} > 10 \text{ kpc}$. This fact, along with a pronounced dip on the metallicity function in the region $[\text{Fe}/\text{H}] \approx -1.0$ also encourages the allocation of metal-rich clusters in the disk subsystem. But, on the other hand, the figure shows that the vast majority of clusters with thick disk kinematics demonstrates $[\text{Fe}/\text{H}] < -1.0$, which is in contradiction with the above-described practice of allocating disk clusters by metallicity. The concentration of metallic clusters to the galactic plane forms a long-known vertical metallicity gradient. The situation is similar with the radial metallicity gradient. In Fig. 1b, it can be seen that at a distance of $z \geq 5 \text{ kpc}$, the main part of the clusters lost by satellite galaxies is located. And in such clusters, the spatial velocities reflect not the dynamic conditions of star formation in a shrinking protogalactic cloud, but only the finite orbits of clusters captured from dwarf satellite galaxies that have disintegrated under the tidal forces of the Galaxy. At the same time, the more massive the parent satellite galaxy, the more flat and elongated its orbit, at which it loses its clusters and stars [15].

²The exception is three distant metal clusters Pal 12, Whiting 1 and Terzan 7, which most likely belonged to the last decayed dwarf galaxy Sagittarius.

4 PROPERTIES OF GLOBULAR CLUSTERS OF DIFFERENT SUBSYSTEMS AND WITH DIFFERENT NATURES

Fig. 2a shows the diagram “azimuthal velocity V_{Θ} – metallicity $[\text{Fe}/\text{H}]$ ” for globular clusters and field stars. Different icons indicate objects of different subsystems of the Galaxy. In contrast to a similar diagram in [5], this one shows clusters with azimuthal velocities significantly different from the solar one in the range $[\text{Fe}/\text{H}] > -1$. Moreover, four metal-rich clusters with retrograde orbits are within 2 kpc from the galactic center, and one—at 4 kpc, whereas 25 metal-poor clusters with $V_{\Theta} < 0$ have an average galactocentric distance of about 8 kpc (15 clusters lie further than 4 kpc). In the diagram “ $V_{\Theta} - [\text{Fe}/\text{H}]$ ”, we have also identified clusters that at different times various authors have considered to belong to formerly decayed dwarf satellite galaxies. Additionally, clusters with galactocentric distances R_G or maximum radii of orbits R_{max} above 15 kpc are noted. As you can see, only one accreted cluster (ω Cen) is not marked, that is, it is closer than this radius. While fifteen other clusters lie far away, their extragalactic origin is not proven. The behavior diagram of “distant” clusters does not agree with the analogous one in MGK19, according to which there is a significant correlation between metallicity and the azimuthal component of velocity. In this work, there are more distant clusters due to the increase in the spatial velocity components and elements of galactic orbits, and there are many distant metal-poor clusters with high azimuthal velocity components. As a result, the correlation noted earlier is disavowed here.

The diagram “morphology of the horizontal branch HBR – metallicity” for our clusters is shown in Fig. 2b. It follows that most of the clusters (but not all) that are currently inside the solar circle ($R_{GC} < 8$ kpc) actually have mostly extremely red or extremely blue horizontal branches. But between these extreme positions, part of the inner clusters lies in a thin layer along the upper envelope in the diagram, while most of the known accreted clusters lie mostly below it (see the inclined line in Fig. 2b drawn “by eye”). However, as can be seen in the diagram, this arrangement is not absolute, and there are exceptions. The probable accreted clusters are most likely also distant clusters (R_{GC} or $R_{max} > 15$ kpc) and clusters with retrograde rotation ($V_{\Theta} < 0.0$). Thirteen of the 26 retrograde clusters lie inside the solar circle. Nine retrograde clusters have extremely blue horizontal branches, five are extremely red, and for ten, branches turned out to be abnormally reddened for their low metallicity. As can be seen in Fig. 2b, all reddened branches really lie in the range between the extreme HBR values in the diagram below the upper envelope. And among the distant clusters all (except three) were metal-poor, whereas the morphology of their horizontal branch can be any. It is generally believed that all metal-poor clusters lying below the narrow upper band can with a high probability be considered as candidates for accreted (see [16]). It seems that this assumption is very plausible, and the redness of the horizontal branches of accreted clusters can be explained. Information on the belonging of clusters to the groups mentioned above is given in the Table.

As we have already noted, recent studies show that within the most massive globular clusters there are several episodes of star formation with supernova explosions that enrich the interstellar medium of the cluster with elements of the iron group. For example, several populations differing in metallicity are found in the largest cluster of Omega Centauri (ω Cen). However, star populations differing in the abundance of helium and CNO elements are also found in less massive clusters (see, for example, paper [17]). It is believed that new, younger star populations in such clusters are formed from chemically contaminated matter ejected by giants of the asymptotic branch of intermediate masses, rapidly rotating massive stars, and also rotating AGB stars of the first generation [18],[19]. Over time, extended horizontal branches form in such clusters, as a result of which their color ceases to correspond to the primary metal-poor chemical composition of the stellar population dominant in number. The authors of [20] showed by numerical modeling that in clusters with a secondary younger population enriched mainly with CNO-elements, the color of the horizontal branch actually becomes more red. At the same time, the Oosterhoff type of cluster changes. As the simulation shows, all this occurs in the initial stages of the cluster’s evolution within one billion years after the last burst of star formation.

In our diagram in Fig. 2b, we can see that of 42 clusters with extremely blue horizontal branches (HBR > 0.85), only eleven are located or have orbit points further than 15 kpc from the galactic center, while 29 clusters are currently inside the solar circle ($R_{GC} < 8$ kpc), and four clusters are between these boundaries. Moreover, among distant clusters, almost all are rather weak in absolute magnitude, that is, their masses are small. This is well illustrated in Fig. 2c, where the diagram “distance from the center of the Galaxy R_G – the absolute magnitude M_V ” for clusters with extremely blue horizontal branches is shown. In addition, the figure highlights distant clusters (R_{GC} or $R_{max} > 15$ kpc). We see that all such clusters have $M_V \geq 8^m.0$ (the exceptions are the distant bright cluster NGC 2419 from Sgr, which has a boundary value HBR = 0.86, and NGC 4833 with a boundary luminosity $-8^m.16$), while all brighter clusters turned out to be close. However, the predominance of low-mass clusters among distant clusters has long been known (see article [21] and references therein), but for extremely blue clusters this regularity is most pronounced. As a result, it turns out that in low-metal clusters, extremely blue horizontal branches are mainly observed near the galactic center and in a small number of distant, relatively low-mass clusters. The reason may be that in both types of clusters, the matter ejected by evolved stars does not remain in the clusters, but is swept away by disturbances of the gravitational potential of the Galaxy. Moreover, in the former, this is due to frequent approachings to the galactic bulge and disk, while in the latter—because of their small mass, unable to hold this matter even at a considerable distance from the galactic center. As a result, the secondary population of them either does not form, or is formed in a small amount. In metal-poor clusters with reddened horizontal branches, all points of the orbits are often outside the solar circle, where disturbances of the gravitational potential of the Galaxy affect less. Perhaps that’s why they have time to form a population of younger stars, distorting the color of their horizontal branches. The described picture is not quite unambiguous, since the third and subsequent populations in some clusters are over-enriched with helium, which leads to the appearance of stars on the horizontal branch on the high-temperature side of the instability band. As a result, the color of the branch shifts to the blue side. A typical example is the cluster M15, which in addition to the normal blue part of the horizontal branch also has the so-called “blue tail” [22]. Verification of the proposed explanation for the existence of a correlation between the color of the horizontal branch and the loss of gas by the cluster requires a detailed analysis of the orbital tracks of the clusters, as well as the use of numerous published data on the individual chemical composition of stars in clusters.

Fig. 2d shows the diagrams of the “azimuthal velocity V_Θ – ratios [Ca,Ti/Fe]” of globular clusters of our sample, for which these parameters are determined, and field stars. Additionally, clusters for which extragalactic origin, that is, considered to be accreted, and distant clusters are indicated on the diagram. The vertical line $V_\Theta = 0$ separates field stars and clusters with retrograde rotation. Field stars are characterized by high (on average) ratios $[\alpha/Fe]$, but with a large spread at small and negative values of the azimuthal velocity and their rapid decrease near the velocity of rotation of the galactic disk at a solar galactocentric distance. In globular clusters with any kinematics, the relations $[\alpha/Fe]$ differ little from each other and do not correlate at all with the azimuthal component of the velocity. And at all values $V_\Theta < V_\odot$ their dispersion is small ($\sigma[\alpha/Fe] \approx 0.1$), however at the velocity of revolution around the galactic center more than solar the dispersion sharply increases (the truth, such clusters are only six, but among them there are clusters both with kinematics of all three subsystems, and clusters of various origin). The high relative abundances of α -elements suggest that almost all clusters were formed, most likely, from interstellar matter not yet enriched with elements of the iron group from type Ia supernova outbursts.

5 ABUNDANCES OF α -ELEMENTS IN GLOBULAR CLUSTERS OF DIFFERENT SUBSYSTEMS AND ORIGIN

Fig. 3a shows the diagram “[Fe/H] – [Ca,Ti/Fe]” for globular clusters of different galactic subsystems and field stars of different nature (details below). The figure shows that clusters belonging to any subsystem by the kinematic criterion, unlike field stars, can have not only different metallicities, but

also different relative abundances of α -elements. In Fig. 3b, where the same diagram is plotted for averaged over four α -elements: magnesium, silicon, calcium and titanium, we see that in general the position of the region occupied by globular clusters relative to field stars has not changed, but the number of clusters decreased. Unlike other diagrams of the figure, on this panel, for comparison, different icons indicate field stars of different galactic subsystems, selected by the kinematic criterion from [13]. It can be seen that the clusters and field stars of the same-name subsystems have a significantly different chemical composition. For genetically connected field stars, that is, formed from a single protogalactic cloud, metallicity can serve as a statistical indicator of their age, since in a closed star-gas system (which in the first approximation can be considered our Galaxy), the total abundance of heavy elements steadily increases over time. As such, we consider field stars with residual velocities $V_{res} > 240 \text{ km s}^{-1}$ (see study [23]), and they are designated by small dark green snowflakes on the diagram. The vast majority of field stars with higher residual velocities (indicated by crosses) have retrograde rotation (see Fig. 2a). All such high-velocity stars can be considered candidates for accreted. Note that metal-poor ($[\text{Fe}/\text{H}] < -1.0$) genetically related field stars are located along the upper half of the strip in Fig. 3a, 3c, 3d. To orient in the figures the broken curves, drawn “by eye”, indicate the lower envelopes for genetically related field stars. The position of our line is in good agreement with paper [24], the authors of which distinguished two populations among metal-poor field stars not by kinematics, but by the relative abundances of α -elements approximately along the boundary $[\alpha/\text{Fe}] \approx 0.3$ and found that the stars of these populations differ not only in chemical composition, but also in kinematics and age. Moreover, they initially looked for evidence that the population with a lower relative abundance of α -elements is of extragalactic origin. Figs. 3a, 3c, 3d show that in genetically related stars, the $[\alpha/\text{Fe}]$ ratios sharply decrease with increasing metallicity, starting from $[\text{Fe}/\text{H}] \approx -1.0$, due to the onset of Ia SNe outbursts in the Galaxy. In globular clusters, this is not observed, and the vast majority of metal-rich clusters lie above the band occupied by field stars. Although a slight decrease in the $[\alpha/\text{Fe}]$ ratios with an increase in metallicity in the range $[\text{Fe}/\text{H}] > -1.0$, is noticeable for them, their positions in the diagram mainly remain in the ratio range $[\alpha/\text{Fe}] > 0.15$, as in less metallic clusters. In this case, clusters belonging by the kinematics to two most numerous galactic subsystems—thick disk and halo—do not show statistically significant differences in positions in Figs. 3a and 3b.

Fig. 3c shows the same “[Fe/H] – [Ca,Ti/Fe]” diagram, but the clusters are distinguished by other signs: accreted clusters, whose membership in the past to decayed satellite galaxies was determined by different authors based on estimates of their positions and spatial movements, distant clusters (R_{GC} or $R_{max} > 15 \text{ kpc}$) and retrograde ones. It can be seen that in the range ($[\text{Fe}/\text{H}] < -1.0$), clusters are located on the diagram so that the lower envelope for genetically related stars is close to the median. It is also seen that, in general, the entire population of accreted clusters, together with candidates for accreted clusters (distant clusters and clusters in retrograde orbits), shows in Fig. 3c a large scatter of the $[\alpha/\text{Fe}]$ ratios. (Moreover, five of the twelve clusters with retrograde orbits were inside the solar circle.) Their spread is much larger than that of genetically related field stars. However, approximately the same wide spread is shown in Fig. 3 by high-velocity ($V_{res} > 240 \text{ km s}^{-1}$) metal-poor field stars that are not genetically related to a single protogalactic cloud and are likely extragalactic in origin. It is possible that a large spread of the $[\alpha/\text{Fe}]$ ratios in such clusters and field stars could be due to the difference in the maximum masses of type II supernovae that enriched the matter of their many parent dwarf galaxies.

In Fig. 3d, solid black circles show clusters that, by any signs, cannot be classified as candidates for accreted ones. We consider such clusters to be genetically related, that is, formed from a single protogalactic cloud. By definition, all 32 such clusters of our sample are located closer than 15 kpc from the galactic center. Moreover, 27 of them, marked in the figure by white triangles inside the circle, generally lie inside the solar circle ($R_{GC} < 8 \text{ kpc}$). And among them are all metal-rich clusters with high ratios $[\text{Ca,Ti}/\text{Fe}]$, some of which most likely belong to the galactic bulge (see [25]). In this diagram, in addition to genetically related clusters, those are also plotted for which belonging to two very massive dwarf galaxies—Sgr and CMa—is considered to be reliably established (see the

list of accreted clusters in MKG19). The figure shows that 21 out of 27 accreted and genetically related clusters in the range $[\text{Fe}/\text{H}] < -1.0$ form a rather narrow band on the diagram, and the lower envelope for genetically related field stars can serve as such for them also. But at the same time, all of these clusters are more closely concentrated to this line than genetically related field stars. (The very low $[\text{Ca}, \text{Ti}/\text{Fe}]$ ratios are shown by two metal-poor clusters from Sgr: a very distant cluster with the only star studied in one work NGC 2419 and Ter 8, however, the relative magnesium abundances in both are high — 0.30 and 0.52, respectively, and the silicon abundance in Ter 8 is 0.38, that is, when all α -elements are taken into account, these clusters also appear near the lower envelope. The situation is similar with the halo cluster NGC 6287, for which $[\text{Si}/\text{Fe}] = 0.55$, a $[\text{Mg}/\text{Fe}] = 0.35$.) But in a more metallic range, both metal-rich clusters (Pal 12 and Ter 7) captured from a dwarf satellite galaxy of Sgr lie below field stars. The metal-poor cluster Rup 106, which is believed to be lost by the rather massive dwarf galaxy CMa [26], is also anomalously low in the diagram. However, the very low relative abundance of α -elements in it along with low metallicity contradicts this assumption. It can be assumed that it was lost by one of the low-mass dwarf satellite galaxies. Provided, of course, that the abundances of α -elements in just two stars of Rup 106 are defined correctly in one article. Note that this cluster is one of the least massive ($M_V = -6^m.35$) metal-poor clusters in the Galaxy and could well be formed in such a dwarf galaxy.

6 ACCRETED GLOBULAR CLUSTERS AND MASSES OF THEIR PARENT GALAXIES

In [27], for 235 stars of the core of the currently destroyed dwarf galaxy Sagittarius (Sgr), the dependence of $[\text{Mg}, \text{Ca}/\text{Fe}]$ on $[\text{Fe}/\text{H}]$ is constructed and it is emphasized that in the low-metal range ($[\text{Fe}/\text{H}] < -1.0$) the sequence of stars from this galaxy coincides with the sequence of field stars of the Galaxy, and with greater metallicity it lies slightly lower than that of field stars. Moreover, the authors of this work note that in the region $[\text{Fe}/\text{H}] > -1.0$ the dependence of the relative abundances of α -elements on metallicity in the Sagittarius galaxy is very similar to that observed in stars of the most massive satellite of the Galaxy—Big Magellanic Cloud. This, in their opinion, also implies a large mass of the Sagittarius galaxy. Indeed, the simulation in [28] of the kinematics of the tidal tail of the stars of the Sagittarius galaxy showed that in order to reproduce the velocity dispersion in the stream from this galaxy, the mass of its dark halo should be $M = 6 \times 10^{10} M_\odot$. The authors of [27] managed to reproduce the observed chemical laws in the parent dwarf galaxy Sagittarius in a model that implies just such a large initial mass and a significant loss of it several billion years ago, starting from its first intersection of the perigalactic of our Galaxy.

In Fig. 3d, among the field stars, the field stars of the so-called Centaurus stream are marked with large gray oblique crosses. It is assumed that all these stars were lost by a dwarf satellite galaxy, the central core of which was the most massive globular cluster Omega Centauri (ω Cen) currently owned by our Galaxy (see article [29] and references therein). Numerical simulation of the dynamic processes occurring during the interaction of the satellite galaxy with the disk and bulge of our Galaxy showed that the capture of the dwarf galaxy core into an elongated retrograde orbit with a small apogalactic radius is quite possible, while the galaxy should be quite massive: of order of $10^9 M_\odot$ [30]. In particular, the results of numerical simulation [31] demonstrated that the orbits of sufficiently massive satellite galaxies are constantly decreasing in size and moving into the galactic plane by dynamic friction. Over time, such galaxies, having acquired very eccentric orbits, almost parallel to the galactic disk, begin to be intensively destroyed by the tidal forces of the Galaxy with each passing perigalactic distance, losing stars with clearly determined orbital energies and angular moments. Therefore, if the observer is between the apogalactic and perigalactic radii of such an orbit, the tidal “tail” from the disrupted galaxy will be observed as a “moving group” of stars with small vertical velocity components and a wide, symmetrical and often bimodal distribution of radial spatial velocity components. Based on the recommendations of the authors of paper [32], in paper [23] from the author’s cumulative catalog of spectroscopic determinations of magnesium abundances

(representative of α -elements) in 800 close F–K–dwarfs of the field [33] by the azimuthal and vertical velocity components in the ranges $-50 \leq V_\theta \leq 0 \text{ km s}^{-1}$ and $|V_z| < 65 \text{ km s}^{-1}$, respectively, stars that were lost by a dwarf galaxy centered on the cluster ω Cen were allocated. It turned out that the isolated 18 stars of the stream did show a rather narrow dependence of $[\text{Mg}/\text{Fe}]$ on $[\text{Fe}/\text{H}]$, characteristic of genetically related stars. Moreover, the position of the “knee point” of the relative magnesium abundance at $[\text{Fe}/\text{H}] \approx -1.3$ dex indicates that the rate of star formation in their parent galaxy was lower than in our Galaxy. Star formation in this galaxy seems to have lasted so long that its most metal-rich stars reached a ratio of $[\text{Mg}/\text{Fe}] < 0.0$ dex, that is, even less than that of the Sun. However, the low value of the maximum metallicity of the stars of this group (only $[\text{Fe}/\text{H}] \approx -0.7$) indicates the cessation of subsequent star formation in their parent galaxy. Most likely, this was due to the beginning of the collapse of the dwarf galaxy. In other words, the chemical composition of the stars of this former galaxy suggests that it did evolve for quite some time (but less than our Galaxy) before collapsing. In this paper, by the same criteria, we isolated the Centauri stream stars from the field star catalog [12] used here. There were also 18 such stars (see Fig. 3d). We see that the behavior of two other α -elements — calcium and titanium — corresponds to the description of the behavior of magnesium according to another catalog. As a result, it turns out that the dependence of $[\alpha/\text{Fe}]$ on $[\text{Fe}/\text{H}]$ in the stars of the Centauri stream is in good agreement with the dependence of accreted clusters in the range $[\text{Fe}/\text{H}] > -1.5$. That is, the assumption is confirmed about the extragalactic origin of at least some high-velocity field stars, that came to us from satellite galaxies of rather large masses .

7 DISCUSSION

Our Galaxy has a complex multicomponent structure, consisting of several subsystems, which are laid out in each other. There are no clear boundaries for subsystems, so their size can be estimated only approximately. Geometric boundaries imply certain dispersions of the velocities of objects belonging to this subsystem. The use of kinematic parameters is considered the most reliable method of stratification of objects by subsystems. It is in this way that the field stars are divided into subsystems of the Galaxy. As the results of this work show, this method is not suitable for globular clusters, since the clusters of different subsystems isolated by kinematics demonstrate chemical properties that are radically different from the properties of the field stars of the same galactic subsystems. In particular, all metal-rich ($[\text{Fe}/\text{H}] > -1.0$) clusters belonging to any subsystem by kinematics are enclosed within rather narrow limits relative to the center and plane of the Galaxy. But in the less metallic range, among the clusters, isolated by kinematics, of both the thick disk and the halo, there are also very distant ones. This is evident in the well-known radial and vertical metallicity gradients in the general population of globular clusters of the Galaxy. It turns out that the traditionally used procedure for isolating the clusters of the thick disk and halo by metallicity is more acceptable. We emphasize that the same contradiction was revealed in our previous work, where the clusters were stratified by velocities from [7]. It turns out that increasing the number and reliability of determining the components of cluster velocities did not lead to its elimination. The difference in the chemical composition of globular clusters and field stars, allocated by the kinematic criterion in the subsystem of the thick disk, indicates, most likely, the lack of correspondence between the subsystems of the same name for these objects. It turns out that the reasons for the formation of these subsystems are different for field stars and globular clusters. Indeed, the high relative abundances of α -elements in metal-rich clusters suggest that they formed within about a billion years after the beginning of star formation. While in the field stars, starting from $[\text{Fe}/\text{H}] = 1.0$, these ratios begin to decrease due to the beginning of the era of mass type Ia supernova outbursts. This suggests that metal-rich field stars are younger than globular clusters of the same metallicity.

However, we note that a similar contradiction, although not so pronounced, between the criteria for belonging to the disk subsystems and the halo by chemical and kinematic properties is also observed in field stars of the RR Lyrae type (see paper [34]). Perhaps not all field lyrids are genetically related

to our Galaxy. In [35] it is proved that some of the field stars got into it from a rather massive captured satellite galaxy shortly after the formation of its own halo (see below for details). By now, some of them may well have become variables of type RR Lyrae. This version is in favor of the fact that the relative abundances of α -elements in the field lyrids undergo a kink in the diagram “[Fe/H] – $[\alpha/\text{Fe}]$ ” at a lower metallicity than field stars. This version is also confirmed by the somewhat lower relative abundances of all α -elements (the above is especially true for titanium) in most metal-rich lyrids with thin disk kinematics (see Figs. 2a – 2d and 3a in work [34]). But then there is a need to explain how such metal-rich stars could have formed at the early stages of evolution in a dwarf galaxy now already, and could have acquired the kinematics of field stars of the thick and thin disk in our Galaxy. Of course, this assumption is very superficial and requires comprehensive justification. Note that in [36] we assumed that relatively young metal-rich field lyrids have increased helium content, leading to faster evolution of stars, and in the vicinity of the Sun they are carried out by radial migration from the central regions of the Galaxy, where such stars have already been found.

Recall that the probabilities of clusters belonging to galactic subsystems are calculated on the basis of residual velocities at galactocentric distances corresponding to current positions. In so doing, it is not taken into account at all how far from the galactic plane the clusters are now. As a result, the vertical components of the residual velocities of clusters located near their apogalactic radii of orbits are underestimated. And this, in turn, can lead to erroneous attribution of such clusters to the disk subsystem. However, our verification showed that, even if clusters located far from the galactic plane were removed from the clusters of the thick disk selected by kinematics, there would still be many metal-poor ones in the subsystem. Moreover, even the maximum distances from the galactic disk in the remaining clusters turned out to be less than 3 kpc. And on the other hand, among metal-rich clusters, there are still many such objects with the kinematics of the halo. That is, the discrepancy between the kinematic and chemical stratification criteria remains.

If we assume that all genetically related globular clusters were formed from the matter of a single protogalactic cloud, then we can assume that the existence of active phases in the evolution of the Galaxy is responsible for such a distinguished position of metal-rich clusters (see the study [3]). The active phase period occurs after massive supernova bursts in the halo, warming up interstellar matter, resulting in a delay in star formation. During this delay, the interstellar matter of the proto-galaxy, already contaminated with heavy elements, mixes, cools and collapses to a smaller size, after which star formation begins again in the Galaxy and disk subsystems are formed. However, in such a scenario, the formation of subsystems in globular clusters does not fit: as can be seen in Fig. 3a–3d, relative abundances of α -elements in almost all studied metal-rich clusters (except three accreted clusters Ter 7, Pal 12 and Rup 106, and two bulge clusters NGC 6528 and NGC 6553) turned out to be high: $[\alpha/\text{Fe}] > 0.15$. The absence of a reliably traceable “knee” on the dependence of $[\alpha/\text{Fe}]$ on $[\text{Fe}/\text{H}]$, as in the field stars, indicates that all the studied clusters were formed before the onset of SNe Ia outbursts, that is, during the first billion years after the start of star formation in the protogalactic cloud. These supernovae enrich the interstellar medium exclusively with atoms of elements of the iron group, as a result of which the $[\alpha/\text{Fe}]$ ratios in the closed star-gas system begin to decrease. As can be determined by the field stars in Fig. 3a – 3d, in the Galaxy this happens at $[\text{Fe}/\text{H}] \approx -1.0$. The same figure shows that within the metallic range, clusters also have a decrease in the relative abundances of α -elements with an increase in metallicity, but the ratios $[\alpha/\text{Fe}]$ for any metallicity remains higher than that of field stars of the thick disk. As a result, the dependence of $[\alpha/\text{Fe}]$ on $[\text{Fe}/\text{H}]$ lies above and parallel to the similar dependence of the field stars. And among them there are clusters of all subsystems allocated by kinematics. As seen in Fig. 3d, what unites the metal-rich clusters is that they all lie inside the solar circle. And even the most remote points of their orbits practically do not go beyond this radius. The estimation of the age of clusters due to its uncertainty does not allow to draw a final conclusion about their nature. In particular, according to estimates of ages from paper [10], they are all younger than 11.5 Gyr. But according to the definitions from paper [11] they are older and appeared simultaneously with the oldest, least metallic clusters. On the other hand, both data show a steady monotonous decrease in the ages of metal-rich clusters with

increasing metallicity. It turns out that more metal-rich clusters with lower relative abundances of α -elements are born mainly later. In this case, we have to agree with the statement that this is due to the beginning of SNe Ia supernovae outbreaks. But then the small ages of metallic clusters from the study [10] seem to be more correct. This behavior of clusters can be put within the framework of the hypothesis about the active phases of Galaxy evolution. Moreover, the higher relative abundances of α -elements for all metal-rich clusters than those of the stars fields, can be explained by the fact that they formed from the interstellar matter, which already collapsed and was enriched with heavy elements after delayed star formation. This interstellar matter of increased density led to an increase in the upper the mass limit of the forming stars, and therefore of the supernovae of the second type, throwing out a greater number of α -elements. In this case, metal-poor, genetically related clusters, the orbits of which also lie almost completely inside the solar circle, should have been born before the onset of the active phase. Indeed, according to [10], the ages of less metallic genetically related clusters are systematically larger. It is possible that already at the time of their birth, the collapse rate of the protogalactic cloud had slowed significantly, which led to the presence of clusters with a “younger” kinematics of the thick disk among them. However, large differences in cluster velocities, according to estimates of various authors, do not exclude the possibility that their errors are significantly underestimated, which could lead to incorrect stratification of some clusters. Thus, based on the hypothesis about the active phases of the evolution of the Galaxy, we can try to give a consistent explanation of the cause of the jump-like change in the volume in the Galaxy occupied by clusters when passing through $[\text{Fe}/\text{H}] \approx -1.0$. Although in this case it is still unclear the existence of clusters with halo kinematics in the range $[\text{Fe}/\text{H}] > -1.0$, the appearance of which can not be attributed to small modern values of errors in the measurement of proper motions and distances to globular clusters.

In our Fig. 3 it can be seen that the entire set of metal-poor ($[\text{Fe}/\text{H}] < -1.0$) globular clusters of the Galaxy occupies on the “[Fe/H] – [α/Fe]” diagram almost the same band along with fast ($V_{\Theta} > 240 \text{ km s}^{-1}$), that is, accreted field stars. Moreover, as follows from the same diagram, the stars of dwarf satellite galaxies [37.39] of our Galaxy, with the same low metallicity, have significantly lower values $[\alpha/\text{Fe}]$. The above indicates that all stellar objects of the accreted halo are remnants of galaxies of higher mass than the current environment of the Galaxy. Differences in the abundances of α -elements between the stellar objects of the Galaxy and the less massive dwarf satellite galaxies surrounding it indicate that the latter did not leave a noticeable stellar trace in it. This conclusion is consistent with the result obtained from a smaller number of globular clusters in [5]. In a recent article [40], based on the discovery of high radial anisotropy of the velocity field in a large sample of halo dwarfs from a vicinity of about 10 kpc from the Sun, it was also concluded that a large-mass satellite accretes to the Galaxy about 8 – 11 Gyr ago. Even more definite conclusions regarding the capture of a massive ($10^9 M_{\odot}$) satellite galaxy by our Galaxy at the early stages of evolution and the formation of a thick disk as a result of its fall due to heating of an already formed thin stellar disk were made in [35]. These conclusions were obtained by analyzing the relative abundances of α -elements and the velocities of several tens of thousands of stars within 15 kpc from the Sun in a sample compiled by cross-identification between the catalogs SDSS–APOGEE DR14 and Gaia DR2.

ACKNOWLEDGMENTS

The authors thank Alexander Chemel for providing spatial velocity components for 115 globular clusters and the rotation curve of his model of the Galaxy.

FUNDING

M. V. A. and G. M. L. thank for the support of the Ministry of Education and Science of the Russian Federation (state assignment No. 3.5602.2017/BCh), and K.V.V. thanks for the support of the Ministry of Education and Science of the Russian Federation (state assignment No. 3.858.2017/4.6).

REFERENCES

- [1] V. A. Marsakov, V. V. Koval' and M. L. Gozha, *Astron. Rep.* **63**, 274 (2019).
- [2] T. V. Borkova and V. A. Marsakov, *Astron. Rep.* **44**, 665 (2000).
- [3] V. A. Marsakov and A. A. Suchkov, *Astron. Rep.* **21**, 700 (1977).
- [4] E. Carretta, IAU Symp. 317, 2015. (Eds. A. Bragaglia, M. Arnaboldi, M. Rejkuba & D. Romano) 97 (2016).
- [5] B. J. Pritzl, K. A. Venn and M. Irwin, *Astron. J.* **130**, 2140 (2005).
- [6] W. E. Harris, *Astron. J.* **112**, 1487 (1996); 2010 edition [arXiv:1012.3224].
- [7] G. M. Eadie and W. E. Harris, *Astrophys. J.* **829**, 108 (2016).
- [8] A. A. Chemel, E. V. Glushkova, A. K. Dambis, A. S. Rastorguev, et al., *Astrophys. Bull.* **73**, 162 (2018).
- [9] A. A. Chemel, (private communication).
- [10] D. A. VandenBerg, *Astrophys. J. Sup.* **129**, 315 (2000).
- [11] M. Salaris and A. Weiss, *Astron. Astrophys.* **388**, 492 (2002).
- [12] K. A. Venn, M. Irwin, M. D. Shetrone, et al., *Astron. J.* **128**, 1177 (2004).
- [13] T. Bensby, S. Feldsing and I. Lundstrom, *Astron. Astrophys.* **410**, 527 (2003).
- [14] O. J. Eggen, D. Linden-Bell and A. Sandage, *Astrophys. J.* **136**, 748 (1962).
- [15] M. G. Abadi, J. F. Navarro and M. Steinmetz, *Monthly Not. Roy. Astron. Soc.* **365**, 747 (2006).
- [16] Y.-W. Lee, H. B. Gim and D. I. Casetti-Dinescu, *Astrophys. J.* **661**, L49 (2007).
- [17] R. G. Gratton, E. Carretta and A. Bragaglia, *Astron. Astrophys. Rev.*, **20**, 50 (2012).
- [18] T. Decressin, G. Meynet, C. Charbonnel, et al., *Astron. Astrophys.* **464**, 1029 (2007).
- [19] P. Ventura and F. D'Antona, *Astron. Astrophys.* **499**, 835 (2009).
- [20] S. Jang, Y.-W. Lee, S.-J. Joo and C. Na, *Monthly Not. Roy. Astron. Soc.* **443**, 15 (2014).
- [21] T. V. Borkova and V. A. Marsakov, *Bull. Spec. Astrophys. Obs.* **54**, 61(2002).
- [22] Y.-W. Lee, P. Demarque and R. Zinn, *Astrophys. J.* **423**, 248 (1994).
- [23] V. A. Marsakov and T. V. Borkova, *Astronomy. Lett.* **32**, 545 (2006).
- [24] P. E. Nissen and W. J. Schuster, *Astron. Astrophys.* **511**, L10 (2010).
- [25] V. V. Bobylev and A. T. Bajkova, *Astron. Rep.* **61**, 551 (2017).
- [26] D. A. Forbes and T. Bridges, *Monthly Not. Roy. Astron. Soc.* **404**, 1203 (2010).
- [27] A. Mucciarelli, M. Bellazzini, R. Ibata, et al., *Astron. Astrophys.* **605**, 46 (2017).
- [28] S. L. J. Gibbons, V. Belokurov, and N. W. Evans, *Monthly Not. Roy. Astron. Soc.* **464**, 794 (2017).

- [29] V. Marsakov, T. Borkova, V. Koval' In: "Variable stars, the Galactic halo and Galaxy formation", B.V.Kurarkin, Centenary Conf. Zvenigorod, Russia, 2009. (Eds. C. Sterken, N. Samus, L. Szabados), Moscow: University Press, 133 (2010).
- [30] T. Tshuchiya, D. Dinescu and V.I. Korchagin, *Astrophys. J. Lett.* **589**, L29 (2003).
- [31] M. G. Abadi, M. G. Navarro, M. Steinmetz and V. R. Eke, *Astrophys. J.* **591**, 499 (2003).
- [32] A. Meza, J. F. Navarro, M. G. Abadi and M. Steinmetz, *Monthly Not. Roy. Astron. Soc.* **359**, 93 (2005).
- [33] T. V. Borkova and V. A. Marsakov, *Astron. Rep.* **49**, 405 (2005).
- [34] V. A. Marsakov, M. L. Gozha, and V. V. Koval', *Astron. Rep.* **62**, 50 (2018).
- [35] J. T. Mackereth, R. P. Schiavon, J. Pfeffer, et al. *Monthly Not. Roy. Astron. Soc.* **482**, 3426 (2018).
- [36] V. A. Marsakov, M. L. Gozha, and V. V. Koval', *Astron. Rep.* **63**, 203 (2019).
- [37] M. D. Shetrone, P. Cote, and W. L. W. Sargent, *Astrophys. J.* **548**, 592 (2001).
- [38] M. Shetrone, K. A. Venn, E. Tolstoy, et al., *Astron. J.* **125**, 684 (2003).
- [39] D. Geisler, V. V. Smith, G. Wallerstein, et al., *Astron. J.* **129**, 1428 (2005).
- [40] V. Belokurov, D. Erkal, N. W. Evans, et al., *Monthly Not. Roy. Astron. Soc.* **478**, 611 (2018).

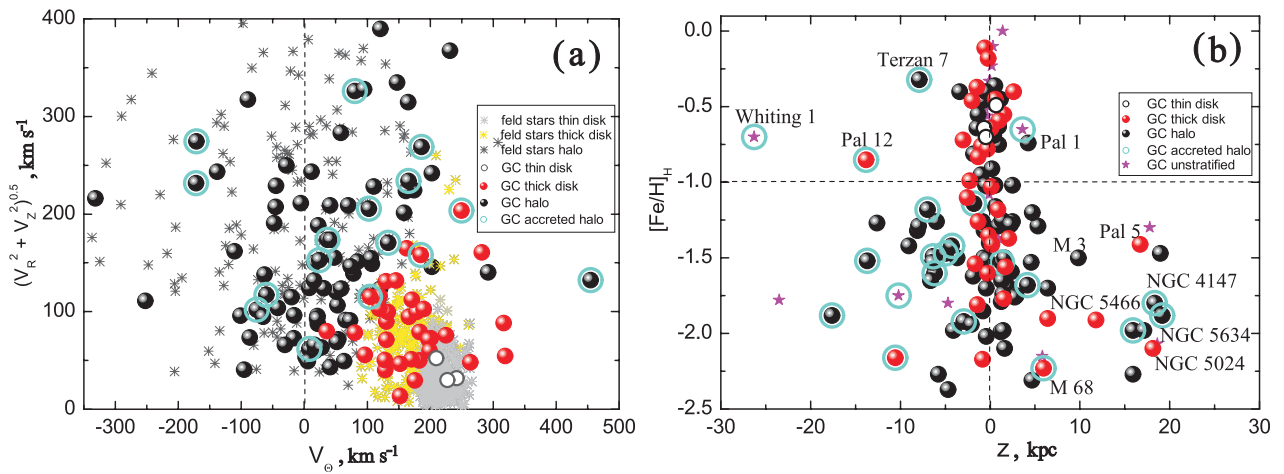


Figure 1: The Tumre diagram for globular clusters and field stars from [12] (a) and the dependence of metallicity on the distance to the galactic plane (b). The field stars are indicated by: light gray snowflakes-the thin disk, yellow-the thick disk, dark gray-the halo. The large circles denoting clusters belonging to the thin disk by kinematic features are empty, those of the thick disk are red, and those of the halo are dark gray. The stars denote unstratified clusters. Circled are clusters known as lost by dwarf galaxies. The values $[\text{Fe}/\text{H}]_H$ are taken from the catalog [6].

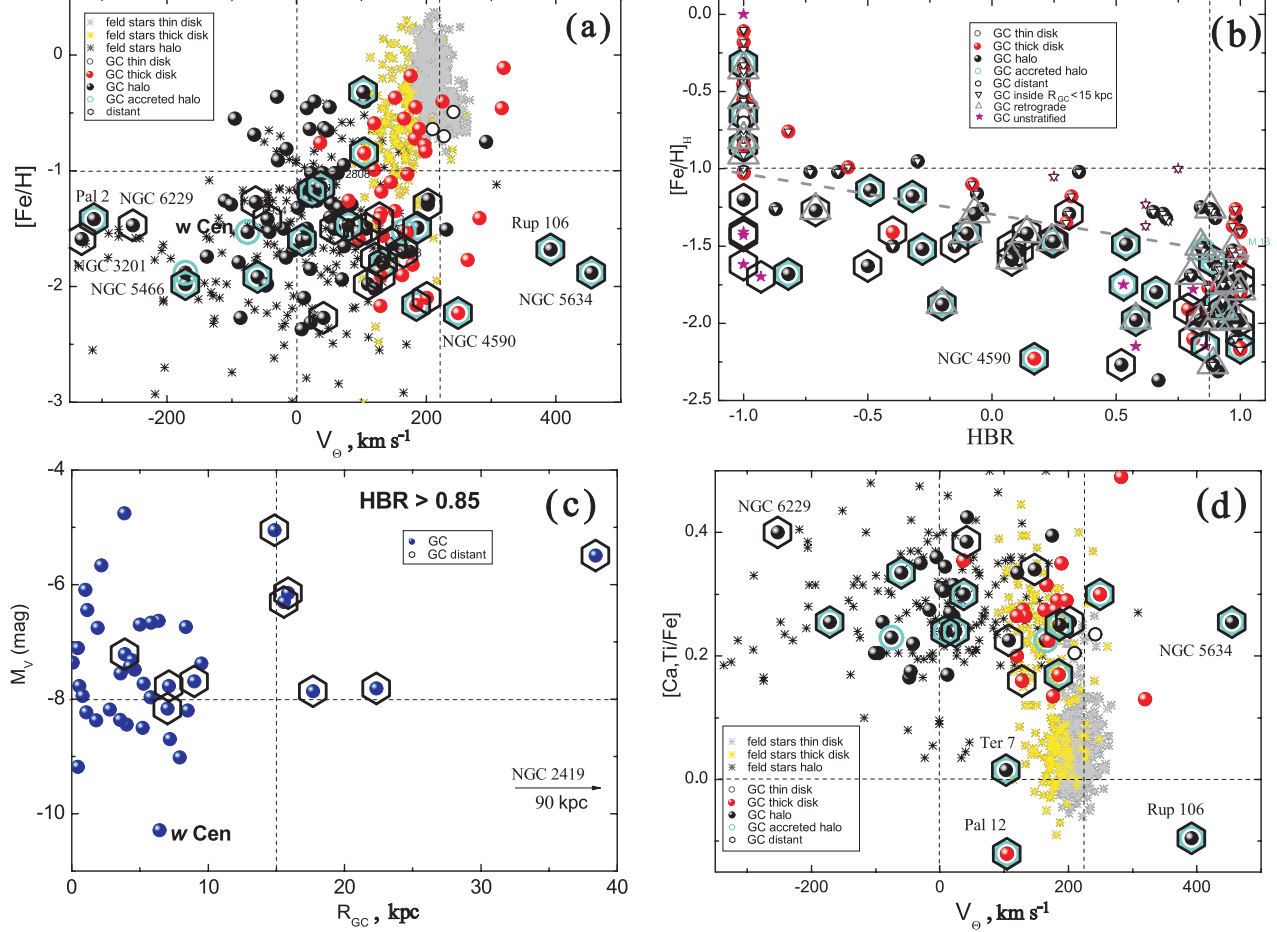


Figure 2: The relation between “spectroscopic metallicity” and rotation speed around the galactic center for the field stars and globular clusters (a); the relation between metallicity from catalog [6] and the color of the horizontal branch clusters (b); the relation between absolute magnitude and galactocentric distance of clusters with extremely blue horizontal branches (c) and the relation between relative abundances of α -elements and rotation speed around the galactic center for field stars and clusters (d). Large hexagons around circles are distant clusters (R_{GC} or $R_{\text{max}} > 15$ kpc); light gray triangles around circles are clusters in retrograde orbits; white triangles inside the icons are clusters lying inside the solar circle ($R_{\text{GC}} < 8$ kpc). The dotted horizontal lines are drawn through $[\text{Fe}/\text{H}] = -1.0$ (a), (b) and $[\alpha/\text{Fe}] = 0.0$ (d); the dotted vertical lines are $V_{\Theta} = 0$ inside the solar circle ($R_{\text{GC}} < 8$ kpc). The dashed horizontal lines are drawn through $[\text{Fe}/\text{H}] = -1.0$ (a), (b) and $[\alpha/\text{Fe}] = 0.0$ (d), and the vertical lines are $V_{\Theta} = 0$ and 220 km s^{-1} (a), (d) and $\text{HBR} = 0.85$ (b); the inclined line is drawn “by eye” and separates the positions of internal and external clusters (b). Other designations are the same as in Fig. 1. The names of clusters, which deviate far from the average for the respective subsystems, are inscribed.

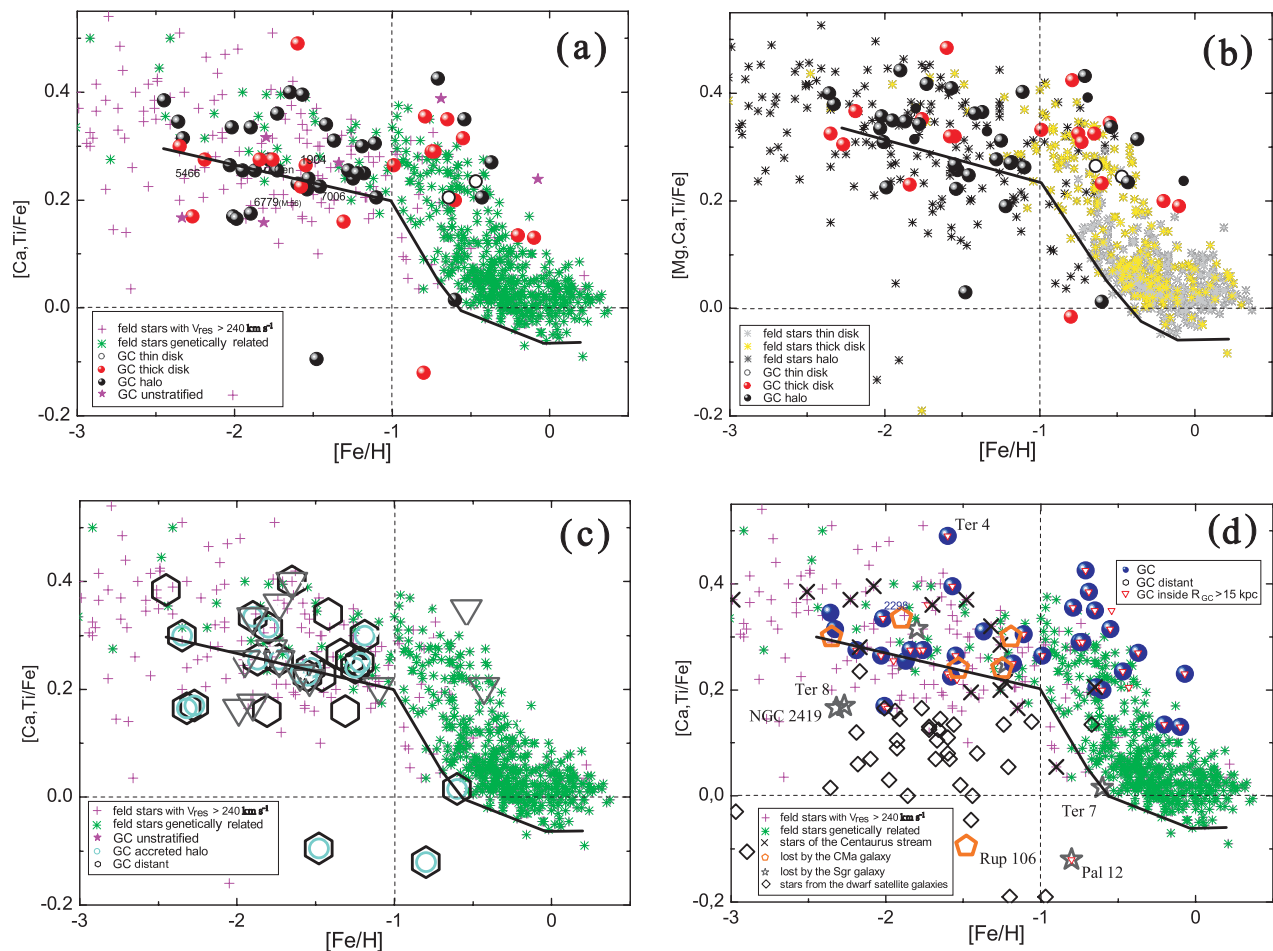


Figure 3: The dependence of the relative abundances averaged over two α -elements (Ca and Ti) (a), (c), (d) and four α -elements (Mg, Ca, Si and Ti) (b) on metallicity for the field stars from paper [12] and globular clusters (due to the lack of silicon abundances in the field stars, they are averaged over three elements). The stars of the field and clusters of different subsystems are indicated as in Fig. 1a (a), (b). Green snowflakes are genetically related field stars with $V_{res} > 240 \text{ km s}^{-1}$, pink crosses are higher-velocity field stars (a) (c), (d); outer and inner clusters in retrograde orbits are indicated as in Figs. 2b and 2c. Large orange pentagons are clusters lost by the CMA galaxy; large gray stars are clusters lost by the Sgr galaxy; diamonds are dwarf satellite galaxy stars from papers [35],[37],[38], large oblique crosses are Centauri stream stars (d). Broken curve line is a drawn “by eye” lower envelope for genetically related field stars (a)–(d).

Table 1: Parameters and labels of globular cluster belonging to subsystems and groups

Name	x , kpc	y , kpc	z , kpc	$[\text{Fe}/\text{H}]_{\text{H}}$	$[\text{Fe}/\text{H}]_{\text{sp}}$	$[\text{Ca}/\text{Ti}/\text{Fe}]$	$[\text{Mg}/\text{Si}/\text{Ca}/\text{Ti}/\text{Fe}]$	V_R , km s^{-1}	V_{Θ} , km s^{-1}	V_Z , km s^{-1}	R_{GC} , kpc	M_V , mag	HBR	sub sys- stem	group
1	2	3	4	5	6	7	8	9	10	11	12	13	14	15	16
NGC 104	1.79	-2.47	-3.03	-0.72	-0.75	0.29	0.43	12.74	182.44	48.35	6.97	-9.42	-0.99	TD	i, t
NGC 288	-0.08	0.04	-8.10	-1.32	-1.37	0.31	0.49	-9.81	2.17	52.37	8.38	-6.74	0.98	H	t
NGC 362	3.00	-4.89	-6.00	-1.26	-1.18	0.25	0.36	111.21	16.50	-100.71	7.21	-8.41	-0.87	H	i, t
NGC 1261	0.09	-9.82	-12.63	-1.27	-	-	-	-115.17	-63.28	76.33	12.80	-7.81	-0.71	H	o, r
NGC 1851	-4.30	-9.02	-7.00	-1.18	-1.25	0.24	0.42	117.79	23.78	-97.21	15.49	-8.33	-0.32	H	o, a
NGC 1904	-7.46	-8.06	-6.18	-1.60	-1.53	0.24	0.34	60.30	8.17	13.86	17.70	-7.86	0.89	H	o, a
NGC 2298	-4.20	-9.28	-2.92	-1.92	-1.90	0.34	0.59	-101.06	-60.01	59.26	15.57	-6.30	0.93	H	o, r, a
NGC 2419	-74.70	-0.50	35.20	-2.15	-2.32	0.17	-	-	-	-	89.90	-9.58	0.86	-	o, a
NGC 2808	1.93	-8.92	-1.81	-1.14	-1.19	0.30	0.36	-173.32	36.61	8.29	10.96	-9.39	-0.49	H	o, a
NGC 3201	0.63	-5.00	0.77	-1.59	-1.49	-	-	-149.15	-331.61	156.54	9.15	-7.46	0.08	H	o, r
NGC 4147	-1.23	-3.98	18.33	-1.80	-	-	-	-29.86	133.33	168.17	10.33	-6.16	0.66	H	a
NGC 4372	2.49	-4.14	-0.84	-2.17	-2.19	0.28	0.49	9.47	128.78	38.88	7.14	-7.77	1.00	TD	i, o, t
NGC 4590	4.04	-7.10	5.94	-2.23	-2.35	0.30	0.43	-203.47	249.44	-7.17	8.28	-7.35	0.17	TD	o, a
NGC 4833	3.23	-4.87	-0.82	-1.85	-2.03	0.27	0.45	71.46	20.96	-63.58	7.02	-8.16	0.93	H	i, t
NGC 5024	2.91	-1.49	18.11	-2.10	-	-	-	-19.56	200.89	-70.16	5.59	-8.70	0.81	TD	o
NGC 5053	2.83	-1.28	15.90	-2.27	-2.45	0.39	-	-25.65	41.15	34.65	5.62	-6.72	0.52	H	o
NGC 5139	3.11	-3.82	1.32	-1.53	-1.60	0.23	-	-63.14	-75.43	-80.04	6.45	-10.29	0.85	H	i, r, a
NGC 5272	1.45	1.32	9.81	-1.50	-1.46	0.23	0.33	-63.77	107.46	-134.72	6.98	-8.93	0.08	H	o
NGC 5286	6.98	-7.86	1.96	-1.69	-1.73	0.36	0.56	-206.77	-5.45	43.78	7.97	-8.61	0.80	H	i, r
NGC 5466	3.48	3.15	15.92	-1.98	-1.73	0.26	0.32	60.37	-171.64	223.68	5.76	-6.96	0.58	H	o, r, a
NGC 5634	15.72	-5.04	19.17	-1.88	-1.87	0.26	0.46	-101.18	454.92	85.01	8.97	-7.69	0.91	H	o, a, t
NGC 5694	25.60	-14.15	17.13	-1.98	-	-	-	-168.29	110.46	-154.06	22.35	-7.81	1.00	H	o
NGC 5824	25.74	-13.37	11.76	-1.91	-	-	-	-130.05	129.51	17.33	21.98	-8.84	0.79	TD	o
NGC 5897	10.48	-3.22	6.41	-1.90	-1.84	0.28	0.31	132.78	162.75	97.81	3.89	-7.21	0.86	TD	i, t
NGC 5904	4.99	0.34	5.32	-1.29	-1.28	0.26	0.37	-209.02	202.43	-121.93	3.33	-8.81	0.31	H	i, o
NGC 5927	6.16	-4.06	0.63	-0.49	-0.47	0.24	0.33	-30.50	242.14	9.54	4.59	-7.80	-1.00	D	i, t
NGC 5946	10.36	-6.58	0.90	-1.29	-	-	-	52.88	84.24	141.70	6.89	-7.20	0.69	H	i, t

Name	x , kpc	y , kpc	z , kpc	$[\text{Fe}/\text{H}]_{\text{H}}$	$[\text{Fe}/\text{H}]_{\text{sp}}$	$[\text{CaTi}/\text{Fe}]$	$[\text{MgSiCaTi}/\text{Fe}]$	V_R , km s^{-1}	V_{Θ} , km s^{-1}	V_Z , km s^{-1}	R_{GC} , kpc	M_V , mag	HBR	sub sys- stem	group
1	2	3	4	5	6	7	8	9	10	11	12	13	14	15	16
NGC 5986	9.23	-3.91	2.36	-1.59	-	-	-	47.97	17.56	-36.09	4.02	-8.44	0.97	H	i, t
NGC 6093	8.14	-1.05	2.90	-1.75	-1.78	0.28	0.46	6.50	-16.49	-72.35	1.06	-8.23	0.93	H	i, r
NGC 6101	10.75	-9.77	-4.12	-1.98	-	-	-	-49.04	-374.20	-171.01	10.07	-6.91	0.84	H	o, r
NGC 6121	2.09	-0.33	0.61	-1.16	-1.11	0.31	0.54	-49.32	5.71	-3.15	6.22	-7.20	-0.06	H	i, t
NGC 6139	9.93	-3.16	1.27	-1.65	-	-	-	43.25	158.63	196.63	3.55	-8.36	0.91	H	i, t
NGC 6144	9.63	-1.36	2.73	-1.76	-	-	-	363.16	120.77	-141.76	1.90	-6.75	1.00	H	i, o
NGC 6171	5.79	0.34	2.46	-1.02	-1.05	-	-	0.63	63.51	-49.10	2.53	-7.13	-0.73	H	i, t
NGC 6205	2.72	4.54	4.58	-1.53	-1.54	0.22	0.30	64.24	-42.12	-81.63	7.19	-8.70	0.97	H	i, r
NGC 6218	4.06	1.14	2.08	-1.37	-1.35	-	-	-12.21	130.14	-89.04	4.40	-7.32	0.97	TD	i, t
NGC 6229	6.29	21.44	18.95	-1.47	-1.65	0.40	-	94.85	-252.56	57.56	21.53	-8.05	0.24	H	o, r
NGC 6235	9.43	-0.18	2.27	-1.28	-	-	-	106.52	52.41	-6.39	1.14	-6.44	0.89	H	i, t
NGC 6254	3.82	1.03	1.69	-1.56	-1.55	0.27	0.43	-84.39	132.81	52.84	4.60	-7.48	0.98	TD	i, t
NGC 6256	9.07	-1.96	0.54	-1.02	-	-	-	-200.40	40.69	58.79	2.11	-6.52	-1.00	H	i, t
NGC 6266	6.60	-0.74	0.85	-1.18	-1.08	-	-	30.09	130.42	64.43	1.85	-9.19	0.32	TD	i, t
NGC 6273	8.37	-0.46	1.39	-1.74	-	-	-	-152.04	-138.65	189.91	0.46	-9.18	0.96	H	i, r
NGC 6284	14.08	-0.41	2.47	-1.26	-	-	-	1.31	-110.79	161.98	5.79	-7.97	0.88	H	i, r
NGC 6287	8.25	0.02	1.61	-2.10	-2.01	0.17	0.41	231.08	11.67	75.95	0.06	-7.36	0.98	H	i, t
NGC 6293	8.71	-0.36	1.20	-1.99	-1.99	0.17	0.30	-144.69	-48.13	-124.02	0.55	-7.77	0.90	H	i, r
NGC 6304	5.96	-0.43	0.56	-0.45	-	-	-	73.80	183.05	28.35	2.38	-7.32	-1.00	TD	i, t
NGC 6316	11.43	-0.56	1.15	-0.45	-	-	-	67.47	51.19	99.83	3.18	-8.35	-1.00	H	i, t
NGC 6333	8.12	0.79	1.54	-1.77	-	-	-	13.66	263.62	46.02	0.81	-7.94	0.87	TD	i, t
NGC 6341	2.45	6.18	4.63	-2.31	-2.33	0.32	0.51	57.63	21.80	65.87	8.51	-8.20	0.91	H	t
NGC 6342	8.94	0.77	1.54	-0.55	-0.55	0.32	0.46	17.35	165.92	-93.08	1.00	-6.44	-1.00	TD	i, t
NGC 6352	5.27	-1.77	-0.70	-0.64	-0.64	0.21	0.35	52.30	209.39	-1.01	3.51	-6.48	-1.00	D	i, t
NGC 6355	9.20	-0.10	0.90	-1.37	-	-	-	-	-	-	1.40	-8.08	0.62	-	i, t
NGC 6356	14.27	1.68	2.59	-0.40	-	-	-	19.37	224.75	73.24	6.20	-8.52	-1.00	TD	i, t
NGC 6362	5.90	-4.04	-2.26	-0.99	-0.99	0.27	0.44	35.37	119.36	96.72	4.71	-6.94	-0.58	TD	i, t

Name	x , kpc	y , kpc	z , kpc	$[\text{Fe}/\text{H}]_{\text{H}}$	$[\text{Fe}/\text{H}]_{\text{sp}}$	$[\text{CaTi}/\text{Fe}]$	$[\text{MgSiCaTi}/\text{Fe}]$	V_R , km s^{-1}	V_{Θ} , km s^{-1}	V_Z , km s^{-1}	R_{GC} , kpc	M_V , mag	HBR	sub sys- tem	sub group
1	2	3	4	5	6	7	8	9	10	11	12	13	14	15	16
NGC 6366	3.28	1.09	0.99	-0.59	-0.60	0.20	0.31	91.01	119.87	-71.95	5.13	-5.77	-0.97	TD	i, t
NGC 6380	10.70	-1.90	-0.60	-0.75	-	-	-	-	-	-	3.30	-7.46	-1.00	-	i, t
NGC 6388	11.06	-2.85	-1.35	-0.55	-0.43	0.21	0.31	-28.39	-95.50	-28.79	3.97	-9.42	-1.00	H	i, r
NGC 6397	2.00	-0.80	-0.46	-2.02	-2.02	0.34	0.48	35.85	120.22	-118.07	6.35	-6.63	0.98	H	i, t
NGC 6401	7.47	0.45	0.52	-1.02	-	-	-	90.11	58.35	84.46	0.95	-7.90	0.35	H	i, t
NGC 6402	7.84	3.06	2.22	-1.28	-	-	-	-69.40	53.76	-17.47	3.09	-9.12	0.65	H	i, t
NGC 6426	17.40	9.30	5.80	-2.15	-	-	-	-	-	-	14.40	-6.69	0.58	-	t
NGC 6440	7.91	1.07	0.53	-0.36	-0.54	0.35	0.45	41.03	-30.69	51.44	1.14	-8.75	-1.00	H	i, r
NGC 6441	9.60	-1.09	-0.85	-0.46	-0.37	0.27	0.42	17.12	16.01	63.81	1.70	-9.64	-1.00	H	i, t
NGC 6453	10.84	-0.81	-0.74	-1.50	-	-	-	-103.73	-20.36	-49.58	2.67	-6.88	0.84	H	i, r
NGC 6496	11.18	-2.37	-2.02	-0.46	-	-	-	-28.90	316.36	-83.41	3.73	-7.23	-1.00	TD	i, t
NGC 6517	10.00	3.50	1.30	-1.23	-	-	-	-	-	-	4.20	-8.28	0.62	-	i, t
NGC 6522	7.70	0.10	-0.50	-1.34	-	-	-	-	-	-	0.60	-7.67	0.71	-	i, t
NGC 6528	7.90	0.20	-0.60	-0.11	-0.10	0.13	0.25	53.85	319.02	8.55	0.60	-6.56	-1.00	TD	i, t
NGC 6535	5.95	3.05	1.23	-1.79	-1.95	0.26	0.47	245.92	-89.78	200.80	3.85	-4.75	1.00	H	i, r
NGC 6539	7.33	2.79	0.93	-0.63	-0.71	0.43	0.58	-130.55	42.16	114.61	2.95	-8.30	-1.00	H	i, t
NGC 6540	3.49	0.20	-0.20	-1.35	-	-	-	8.42	151.86	10.61	4.82	-5.38	0.30	TD	i, t
NGC 6541	7.13	-1.35	-1.44	-1.81	-1.76	0.28	0.47	95.40	178.63	-28.83	1.78	-8.37	1.00	TD	i, t
NGC 6544	2.49	0.25	-0.10	-1.40	-	-	-	2.65	51.43	-69.10	5.82	-6.66	1.00	H	i, t
NGC 6553	4.67	0.43	-0.25	-0.18	-0.20	0.14	0.27	9.61	175.77	27.95	3.65	-7.77	-1.00	TD	i, t
NGC 6558	6.36	0.02	-0.67	-1.32	-	-	-	137.66	78.12	-19.88	1.94	-6.46	0.70	H	i, t
NGC 6569	8.44	0.07	-0.99	-0.76	-0.79	0.36	0.57	-45.09	35.89	-66.22	0.16	-8.30	-0.82	TD	i, t
NGC 6584	11.87	-3.82	-3.67	-1.50	-	-	-	136.53	58.05	-248.00	5.23	-7.68	-0.15	H	i, o
NGC 6624	7.80	0.40	-1.10	-0.44	-0.69	0.39	0.52	-	-	-	1.20	-7.49	-1.00	-	i, t
NGC 6626	5.62	0.77	-0.55	-1.32	-	-	-	-27.07	65.64	-87.47	2.79	-8.18	0.90	H	i, t
NGC 6637	8.06	0.24	-1.46	-0.64	-	-	-	-76.22	20.18	53.10	0.34	-7.64	-1.00	H	i, t

Name	x , kpc	y , kpc	z , kpc	$[\text{Fe}/\text{H}]_{\text{H}}$	$[\text{Fe}/\text{H}]_{\text{sp}}$	$[\text{Ca}/\text{Ti}/\text{Fe}]$	$[\text{Mg}/\text{Si}/\text{Ca}/\text{Ti}/\text{Fe}]$	V_R , km s^{-1}	V_{Θ} , km s^{-1}	V_Z , km s^{-1}	R_{GC} , kpc	M_V , mag	HBR	sub sys- stem	group
1	2	3	4	5	6	7	8	9	10	11	12	13	14	15	16
NGC 6638	8.06	1.12	-1.02	-0.95	-	-	-	81.56	72.57	40.62	1.14	-7.13	-0.30	H	i, t
NGC 6642	7.44	1.29	-0.85	-1.26	-	-	-	104.54	31.04	-66.93	1.55	-6.77	-0.04	H	i, t
NGC 6652	9.21	0.25	-1.85	-0.81	-	-	-	-91.84	-16.04	28.43	0.94	-6.68	-1.00	H	i, r
NGC 6656	3.13	0.54	-0.42	-1.70	-1.57	0.40	0.55	172.23	174.22	-143.79	5.20	-8.50	0.91	H	i, t
NGC 6681	8.48	0.42	-1.88	-1.62	-	-	-	137.00	161.44	-176.82	0.46	-7.11	0.96	H	i, t
NGC 6712	6.04	2.86	-0.50	-1.02	-	-	-	118.47	22.38	-146.65	3.65	-7.50	-0.62	H	i, t
NGC 6715	25.29	2.48	-6.38	-1.49	-1.22	0.25	0.25	211.70	186.21	165.82	17.17	-10.01	0.54	H	i, o, a, t
NGC 6717	6.80	1.55	-1.34	-1.26	-	-	-	-55.34	80.35	55.64	2.16	-5.66	0.98	TD	i, t
NGC 6723	8.21	0.01	-2.56	-1.10	-	-	-	123.07	145.44	-48.05	0.09	-7.84	-0.08	TD	i, t
NGC6749	6.21	4.54	-0.30	-1.60	-	-	-	-0.25	96.05	55.77	5.00	-6.70	1.00	TD	i, t
NGC 6752	3.22	-1.40	-1.69	-1.54	-1.58	0.23	0.43	-14.00	170.39	49.27	5.27	-7.73	1.00	TD	i, t
NGC 6760	5.88	4.29	-0.50	-0.40	-	-	-	143.62	105.55	-57.55	4.93	-7.86	-1.00	H	i, t
NGC 6779	4.50	8.70	1.44	-1.98	-1.90	0.18	-	166.86	-45.45	122.97	9.50	-7.38	0.98	H	i, r
NGC 6809	4.81	0.74	-2.09	-1.94	-1.93	-	-	-204.06	69.94	-45.00	3.57	-7.55	0.87	H	i, t
NGC 6838	2.08	3.17	-0.30	-0.78	-0.73	0.29	0.41	15.94	196.98	69.77	6.98	-5.60	-1.00	TD	i, t
NGC 6864	15.54	5.75	-7.99	-1.29	-1.10	0.21	0.35	-95.59	-101.44	-8.19	9.25	-8.55	-0.07	H	r
NGC 6934	8.83	11.35	-4.92	-1.47	-	-	-	-320.11	80.44	61.31	11.36	-7.46	0.25	H	o, a
NGC 6981	11.56	8.14	-9.07	-1.42	-	-	-	-162.16	-44.68	161.76	8.77	-7.04	0.14	H	o, r
NGC 7006	17.20	34.80	-13.70	-1.52	-1.55	0.23	0.36	-180.81	165.32	148.41	38.50	-7.68	-0.28	H	o, a
NGC 7078	3.83	8.21	-4.68	-2.37	-2.36	0.35	0.53	102.63	7.87	-70.09	9.35	-9.17	0.67	H	t
NGC 7089	5.52	7.42	-6.66	-1.65	-	-	-	102.76	73.79	-103.95	7.93	-9.02	0.92	H	i, t
NGC 7099	4.81	2.47	-5.76	-2.27	-2.31	-	-	-0.43	-86.39	73.72	4.28	-7.43	0.89	H	i, r
NGC 7492	7.00	9.40	-23.50	-1.78	-1.81	0.16	0.42	-	-	-	25.30	-5.77	0.81	-	o
1636-283	7.36	-1.05	1.59	-1.50	-	-	-	35.09	15.86	127.32	1.41	-3.97	-0.40	H	i, t
2MS-GC01	3.50	0.70	0.00	-	-	-	-	-	-	-	4.50	-	-	-	i, t
2MS-GC02	4.90	0.80	-0.10	-1.08	-	-	-	-	-	-	3.20	-	-	-	i, t

Name	x , kpc	y , kpc	z , kpc	$[\text{Fe}/\text{H}]_{\text{H}}$	$[\text{Fe}/\text{H}]_{\text{sp}}$	$[\text{Ca}/\text{Ti}/\text{Fe}]$	$[\text{MgSiCaTi}/\text{Fe}]$	V_R , km s^{-1}	V_{Θ} , km s^{-1}	V_Z , km s^{-1}	R_{GC} , kpc	M_V , mag	HBR	sub sys- tem	group
1	2	3	4	5	6	7	8	9	10	11	12	13	14	15	16
AM1	-16.50	-80.10	-92.30	-1.70	-	-	-	-	-	-	124.60	-4.71	-0.93	-	o
AM4	20.70	-17.20	17.80	-1.30	-	-	-	-	-	-	27.80	-1.60	-	-	o
Arp 2	26.40	4.00	-10.20	-1.75	-1.80	0.32	0.50	-	-	-	21.40	-5.29	0.53	-	o
BH 176	16.10	-9.90	1.40	0.00	-	-	-	-	-	-	12.90	-4.35	-1.00	-	t
BH 261	6.50	0.40	-0.60	-1.30	-	-	-	-	-	-	1.70	-	-	-	i, t
Djorg 1	9.18	-0.53	-0.40	-1.51	-	-	-	-281.58	231.15	236.16	1.03	-6.26	-	H	i, t
Djorg 2	13.77	0.67	-0.60	-0.65	-	-	-	-128.51	47.23	87.17	5.51	-6.98	-1.00	H	i, t
E3	1.50	-3.67	-1.37	-0.83	-	-	-	-16.74	198.76	-57.46	7.73	-2.77	-	TD	i, t
Eridanus	-53.20	-41.70	-59.50	-1.43	-	-	-	-	-	-	95.00	-5.14	-1.00	-	o
ESO-SC06	20.40	-4.70	-4.70	-1.80	-	-	-	-	-	-	14.00	-	-	-	t
FSR 1735	9.10	-3.50	-0.30	-	-	-	-	-	-	-	3.70	-	-	-	i, t
GLIMPSE01	3.60	2.20	0.00	-	-	-	-	-	-	-	4.90	-	-	-	i, t
GLIMPSE02	5.40	1.40	-0.10	-0.33	-	-	-	-	-	-	3.00	-	-	-	i, t
HP 1	8.20	-0.40	0.30	-1.00	-	-	-	-	-	-	0.50	-6.44	0.75	-	i, t
IC 1257	22.67	6.73	6.40	-1.70	-	-	-	125.78	165.04	288.49	15.87	-6.15	1.00	H	o,
IC 1276	8.59	3.44	0.92	-0.75	-	-	-	-37.49	292.05	135.07	3.45	-6.67	-1.00	H	i, t
IC 4499	10.46	-13.70	-6.43	-1.53	-	-	-	-229.21	94.99	-234.48	13.87	-7.33	0.11	H	o
Ko 1	-2.50	-15.70	45.60	-	-	-	-	-	-	-	49.30	-	-	-	o
Ko 2	-30.20	-8.20	15.00	-	-	-	-	-	-	-	41.90	-	-	-	o
Liller 1	8.20	-0.70	0.00	-0.33	-	-	-	-	-	-	0.80	-7.63	-1.00	-	i, t
Lynga 7	6.80	-4.10	-0.40	-1.01	-	-	-	-	-	-	4.30	-	-1.00	-	i, t
Pal 1	-6.80	8.10	3.60	-0.65	-	-	-	-	-	-	17.20	-2.47	-1.00	-	o, a
Pal 10	3.60	4.70	0.30	-0.10	-	-	-	-	-	-	6.40	-5.79	-1.00	-	i, t
Pal 11	10.31	6.40	-3.38	-0.40	-	-	-	63.32	27.34	-1.15	6.71	-6.86	-1.00	H	i, t
Pal 12	10.85	6.39	-13.83	-0.85	-0.80	-0.12	-0.02	114.64	104.40	-11.88	6.88	-4.48	-1.00	TD	i, o, a
Pal 13	1.00	19.10	-17.60	-1.88	-	-	-	255.33	-171.54	-100.45	26.90	-3.74	-0.20	H	o, r, a
Pal 14	49.70	27.30	51.40	-1.62	-1.34	0.27	0.44	-	-	-	71.60	-4.73	-1.00	-	o
Pal 15	38.90	13.30	18.60	-2.07	-	-	-	-	-	-	38.40	-5.49	1.00	-	o

Name	x , kpc	y , kpc	z , kpc	$[\text{Fe}/\text{H}]_{\text{H}}$	$[\text{Fe}/\text{H}]_{\text{sp}}$	$[\text{CaTi}/\text{Fe}]$	$[\text{MgSiCaTi}/\text{Fe}]$	V_R , km s^{-1}	V_{Θ} , km s^{-1}	V_Z , km s^{-1}	R_{GC} , kpc	M_V , mag	HBR	sub sys- tem	group
1	2	3	4	5	6	7	8	9	10	11	12	13	14	15	16
Pal 2	-26.20	4.37	-4.24	-1.42	-	-	-	26.47	-312.64	746.70	34.78	-8.01	-0.10	H	o, r, a
Pal 3	-34.30	-59.70	61.70	-1.63	-1.42	0.34	0.48	-262.14	147.14	208.07	95.70	-5.70	-0.50	H	o
Pal 4	-31.40	-12.90	103.20	-1.41	-	-	-	-	-	-	111.20	-6.02	-1.00	-	o
Pal 5	16.20	0.20	16.70	-1.41	-1.31	0.16	-	-48.01	127.88	-15.66	18.60	-5.17	-0.40	TD	o
Pal 6	6.69	0.25	0.21	-0.91	-	-	-	-226.31	-28.69	106.27	1.63	-6.81	-1.00	H	i, r
Pal 8	11.94	3.00	-1.47	-0.37	-	-	-	-40.69	152.12	22.66	4.72	-5.52	-1.00	TD	i, t
Pyxis	-5.77	-37.78	4.69	-1.20	-	-	-	-83.14	682.67	82.20	40.31	-5.75	-1.00	H	o
Rup 106	10.35	-17.31	4.17	-1.68	-1.48	-0.10	0.04	6.09	391.65	-464.16	17.43	-6.35	-0.82	H	o, a
Terzan 1	6.49	-0.28	0.11	-1.03	-	-	-	-70.36	170.75	-87.41	1.83	-4.90	-1.00	TD	i, t
Terzan 10	5.80	0.50	-0.20	-1.00	-	-	-	-	-	-	2.30	-6.31	-1.00	-	i, t
Terzan 12	4.70	0.70	-0.20	-0.50	-	-	-	-	-	-	3.40	-4.14	-1.00	-	i, t
Terzan 2	9.47	-0.61	0.38	-0.69	-	-	-	82.25	-65.32	47.20	1.32	-5.27	-1.00	H	i, r
Terzan 3	25.18	-6.71	4.22	-0.74	-	-	-	-176.64	513.67	277.94	18.17	-4.61	-1.00	H	-
Terzan 4	7.20	-0.50	0.20	-1.41	-1.60	0.49	0.65	-135.13	281.86	-87.10	1.00	-6.09	1.00	TD	i, t
Terzan 5	6.90	0.50	0.20	-0.23	-0.07	0.23	0.32	-	-	-	1.20	-7.87	-1.00	-	i, t
Terzan 6	6.80	-0.20	-0.30	-0.56	-	-	-	-	-	-	1.30	-7.67	-1.00	-	i, t
Terzan 7	21.57	1.28	-7.89	-0.32	-0.60	0.02	0.02	204.03	102.80	24.39	13.33	-5.05	-1.00	H	o, a
Terzan 8	22.99	2.32	-10.56	-2.16	-2.27	0.17	0.40	157.28	184.87	-15.49	14.87	-5.05	1.00	TD	o, a
Terzan 9	7.10	0.40	-0.20	-1.05	-	-	-	-	-	-	1.10	-3.85	0.25	-	i, t
Ton 2	7.78	-1.26	-0.47	-0.70	-	-	-	-24.05	227.11	-17.70	1.36	-6.14	-1.00	D	i, t
UKS1	7.47	0.67	0.10	-0.64	-0.65	0.35	0.43	60.48	189.39	83.13	1.07	-6.88	-1.00	TD	i, t
Whiting 1	-13.90	4.70	-26.30	-0.70	-	-	-	-	-	-	34.50	-	-	-	o, a

Belonging of clusters to galactic subsystems and groups:

T, TD and H – thin disk, thick disk and halo, respectively;

i – internal: located at a distance (or apogalactic radii of their orbits) less than 8 kpc;

o – distant: located at a distance or have radii of orbits greater than 15 kpc;

r – retrograde: the azimuthal components of their velocity are less than zero;

a – accreted: the works of other authors prove their extragalactic origin;

t – genetically related: the clusters not falling into any of the last three groups.